# Flow-Induced Vibration of Helical Coil Compression Springs

F.E. Stokes
*Babcock and Wilcox, Research and Development Division, 1562 Beeson Street, Alliance, Ohio 44601, U.S.A.*
R.A. King
*Babcock and Wilcox, Nuclear Power Generation Division, P.O. Box 1260, Lynchburg, Virginia 24505, U.S.A.*

SUMMARY

Helical coil compression springs are used in some nuclear fuel assembly designs to maintain holddown and to accommodate thermal expansion. In the reactor environment, the springs are exposed to flowing water, elevated temperatures and pressures, and irradiation. Flow parallel to the longitudinal axis of the spring may excite the spring coils and cause vibration. The purpose of this investigation was to determine the flow-induced vibration (FIV) response characteristics of helical coil compression springs.

Experimental tests indicate that a helical coil spring responds like a single circular cylinder in cross-flow. Two FIV excitation mechanisms control spring vibration. Namely:

1) Turbulent Buffeting causes small amplitude vibration which increases as a function of velocity squared.

2) Vortex Shedding causes large amplitude vibration when the spring natural frequency and Strouhal frequency coincide.

Several methods can be used to reduce or to prevent vortex shedding large amplitude vibrations. One method is compressing the spring to a coil pitch-to-diameter ratio of 2 thereby suppressing the vibration amplitude. Another involves modifying the spring geometry to alter its stiffness and frequency characteristics. These changes result in separation of the natural and Strouhal frequencies.

With an understanding of how springs respond in the flowing water environment, the spring physical parameters can be designed to avoid large amplitude vibration.

## 1. Introduction

Nuclear fuel assemblies are subject to hydraulic forces generated by primary coolant flow during reactor operation. These forces may be sufficient to overcome the fuel assembly weight thereby allowing the assembly to lift off of its support. Since fuel assemblies are generally made of different materials than are the reactor vessel, thermal and radiation growth rates differ. Thus, fixed support conditions cannot be employed to maintain the fuel assembly position during operation.

Helical coil springs or leaf springs are inserted in the fuel assemblies to provide a positive holddown margin against the opposing coolant flow forces. Differences in thermal and radiation growth of the reactor components are accommodated by spring compression changes to maintain the fuel assembly holddown. A single spring or a cluster of springs may be used to provide the holddown capability.

Designing springs to handle the holddown function requires that the mechanical and metallurgical properties of the spring material be evaluated to ensure that the spring can withstand the corrosive reactor environment, be relatively unaffected by radiation, and exhibit acceptable creep levels over the design life of 3 - 5 years.

The spring design specifications are dependent on the accessible space in the fuel assembly and the load and deflection requirements to maintain holddown. If the spring is located in a flow path, its dynamic characteristics must also be evaluated. As with any object immersed in a flowing medium, the spring can be excited by the applied flow forces and will respond in a vibratory manner.

The purpose of this investigation was to experimentally determine the flow-induced vibration characteristics of helical coil compression springs in a flowing water medium. This study identifies the mechanisms causing spring vibration and offers methods to avoid large amplitude vibration. The results of this work has been incorporated into Babcock & Wilcox's helical coil holddown spring design guide.

## 2. Apparatus

### 2.1 Springs

Five different helical coil compression spring designs were evaluated. Table 1 lists the primary specifications of these springs. The major portion of the experimental investigation was conducted on Spring No. 1. This design laid the groundwork for the FIV mechanism determination while the remaining designs were tested to evaluate various parametric effects on the spring response. Figure 1 is a photograph of the tested springs.

### 2.2 Flow Test Equipment

An aluminum and glass flow channel was fabricated to test individual springs over a range of compressed heights and flow rates. The spring flow channel was installed horizontally in one of several flow test facilities at the Babcock & Wilcox Alliance Research Center. This cold flow test facility has flow capabilities ranging from 200 to 3500 gpm at temperatures up to 170°F. The flow channel is shown in Figure 2. The spring was supported between a section of a fuel assembly upper end fitting grillage and a compression device with positioning lugs. A rack and pinion drive system enables changing compression during operation. The glass sideplates permit visualization of the spring motion.

Due to the characteristics of the springs, strain gages or accelerometers could not be attached to obtain the response signal. Application of these devices and their lead wires disturbed the boundary layer and reduced or eliminated motion. To avoid affecting the response, visual and non-contact techniques were utilized to characterize the spring motion.

A General Dynamics Strobatac strobe light was used to provide general spring motion information. The strobe frequency was varied until it approached the spring response frequency. As this occurred, the spring motion appeared to slow down and eventually stop, indicating a lock-in with the spring frequency. Amplitudes of vibration were estimated by observing the reduced speed motion in reference to a tenth-inch grid network etched on the glass windows.

More accurate, permanent documentation of the spring response was obtained using high-speed photography techniques. A Hycam high-speed motion picture camera, which has a film

speed of 1000 frames per second and a frequency reference timing light, was used to photograph the spring response under the flowing water conditions. This method had several disadvantages. Several days elapsed between the time of filming and return of the developed film. As such, improper lighting or focus could not be ascertained expeditiously, thus leading to extended periods of time to rerun tests. Analysis of the film also was very time consuming and cost inefficient.

The developed film was analyzed on a frame-by-frame basis using a Vanguard Motion Analyzer. The positions of targets on the spring mid-coil and a reference on the flow channel were determined for each frame studied. Further reduction of the film data was performed using a computer program that computes the frequency and relative motion amplitude of the spring from the Vanguard analyzer data. In addition, an amplitude histogram fitted with a Gaussian distribution identifies the level of randomness or periodicity in the spring response. Displacement time history plots are generated by approximating the data with a trigonometric series. The output of the calculated polynomial is plotted to indicate the relative motion of the spring.

## 3. Flow Testing

### 3.1 FIV Mechanism Determination

The No. 1 Design Spring was inserted in the single spring test section and compressed to a height of approximately 4 inches. The flow velocity through the test facility was varied from 3 to 25 ft/sec in 1 ft/sec increments. At each condition, the motion of the spring was visually observed using the strobe light. With flow velocities causing motion of the spring, the corresponding motion direction and amplitude were recorded. Specific flow velocities within the range were chosen for further vibration analysis using the high-speed photography techniques.

The final form of the data from the films, showing the relationship between the spring response amplitude as a function of flow velocity, is illustrated in Figure 3. The following paragraphs describe the spring motion as the flow velocity range was traversed.

No motion was observed at the lowest flow velocity. As the velocity was increased, spring vibration began. At slightly more than 4 ft/sec, the coil amplitude increased in the direction of flow (axial). The motion was characterized by the three middle coils vibrating in-phase at a frequency of 74 Hz which corresponds to the spring natural frequency in water.

As the velocity increased beyond 6 ft/sec, the resulting vibration amplitude decreased and the predominant frequency response became less pronounced. From about 8 to 11 ft/sec, the spring response became random and increased in proportion to the velocity squared. The vibration amplitude rose quickly as the flow approached 13 ft/sec and peaked near 16 ft/sec. The spring frequency response was 111 Hz -- the lateral natural frequency of the spring in water.

At this apparent resonant vibration condition, the spring coils were moving out-of-phase with the motion in the axial direction towards the center of the spring from the ends. Lateral movement of the spring coils in the vertical direction perpendicular to the flow was also observed. As the coils vibrated laterally, they also appeared to have a radial component.

As the flow was increased beyond 16 ft/sec, the spring motion decreased. However, over the 13 to 19 ft/sec velocity range, the spring motion was predominantly lateral. Beyond 20 ft/sec, the frequency response was primarily random, while the coil amplitude continued to decrease.

The sharp increases in amplitude occurred as the flow response frequencies matched the axial and lateral spring natural frequencies and were followed by amplitude decreases as the response frequency changed. This type of response is characteristic of the vortex shedding flow-induced vibration mechanism. For simplicity, the spring was assumed to represent a single circular cylinder, with a diameter corresponding to the wire diameter, in cross-flow. The velocity at which vortex shedding should occur in the lateral (lift) direction is calculated using [1]:

$$V = \frac{f_s d}{12S} \qquad (1)$$

where:

$V$ = vortex shedding velocity, ft/sec

$f_s$ = vortex shedding or Strouhal frequency, Hz

$d$ = spring wire diameter, in.

$S$ = Strouhal number

The axial direction velocity includes a divisor of 2 in Eq. (1).

For this analysis, the vortex shedding frequency was equated to the 4-inch compressed height natural frequency of the spring in water. Over the flow velocity range tested, the Reynolds number varied from 11,000 to 90,000. This corresponds to a Strouhal number of 0.19 to 0.2. From Eq. (1), the velocities at which vortex shedding should occur for axial and lateral vibration are approximately 5.4 and 16 ft/sec, respectively. These velocities agree with the measured peak coil amplitude velocities indicating vortex shedding is the mechanism causing the large amplitude spring vibration.

At the intermediate flow rates between the large peaks, the vibration amplitudes increased as a function of velocity squared. The spring vibration was primarily random, with the frequency response in a band surrounding the Strouhal frequency. This corresponds to vibration induced by turbulent buffeting.

3.2 Analytical Model

The effects of vortex shedding on the vibration of circular cylinders have been evaluated numerous times. The analysis procedure for circular cylinders was applied to the helical coil compression spring.

The dynamic fluid force acting on the spring is composed of a drag and a lift component. The drag force acts in the direction of flow, while the lift force acts in the direction transverse to the flow. The drag and lift forces exerted on the spring are given by [2]:

$$F_D = C_D \frac{1}{2} \frac{\rho}{g} \frac{Av^2}{144} \qquad F_L = C_L \frac{1}{2} \frac{\rho}{g} \frac{Av^2}{144} \tag{2}$$

where:

$F_D$, $F_L$ = fluctuating drag and lift forces, lb

$C_D$, $C_L$ = fluctuating drag and lift coefficients

$\rho$ = density of fluid, lbm/ft$^3$

$g$ = gravitational constant, lbm ft/lbf sec$^2$

$A$ = projected area per linear length of spring, in$^2$

$v$ = coolant flow velocity, ft/sec

Lienhard summarized the studies performed by others and found that the fluctuating drag coefficient, $C_D$, ranges from 0.1 to 0.2 [3]. A value of $C_D = 0.2$ was used in this analysis. The available data for the oscillating lift coefficient, $C_L$, is scattered between 0.1 and 1.5 over a Reynolds number range of $10^3$ to $10^6$ [2]. For this study, a lift coefficient of 0.75 was chosen.

At a given velocity, the maximum zero-to-peak mid-coil displacement can be calculated from:

$$Y_{max} = \frac{F}{K} |H(f)| \tag{3}$$

where:

$F$ = drag or lift force, lb

$K$ = axial or lateral spring rate, lb/in

$|H(f)|$ = magnification factor

The magnification factor is determined using the expression:

$$|H(f)| = \frac{1}{\sqrt{\left(1 - \left(\frac{f_s}{f_n}\right)^2\right)^2 + \left(2\xi \frac{f_s}{f_n}\right)^2}} \qquad (4)$$

where:

$f_s$ = vortex shedding frequency

$f_n$ = spring natural frequency

$\xi$ = damping factor

The vortex shedding frequencies are obtained from Eq. (1) with the factor of 2 applied for the axial direction. The values of damping, axial spring rate, and lateral spring rate were determined from in-air tests. The spring vibration amplitude was calculated over the 3 to 25 ft/sec flow velocity range. Figure 4 illustrates the predicted vibration amplitudes for Spring No. 1 at a 4-inch compressed height. Superimposed on the plot is the measured response curve from Figure 3. The predicted response is very similar to the measured response except for a slight shift in the axial resonance velocity and a narrowing of the amplitude bandwidth. This curve further substantiates vortex shedding as the flow-induced vibration mechanism causing large amplitude vibration of helical coil compression springs.

## 4. Additional Studies

Additional testing was performed for further evaluation of the flow-induced vibration characteristics of helical coil compression springs. The additional studies include:

1) Effect of compressed height on spring response.

2) Alternate designs.

### 4.1 Compressed Height Effects

The previously described flow test was repeated for six compressed heights of Spring No. 1. The flow velocity was varied from approximately 8 to 25 ft/sec to evaluate the lateral response. Figure 5 illustrates the spring amplitudes as a function of flow velocity for the six compressed heights. The figure indicates the spring continues to vibrate at resonance through the flow range at which the Strouhal and natural frequencies coincide. Variations in amplitude associated with compressed height are expected from the analytical model. The parameters contributing most significantly to the predicted amplitude are the lateral stiffness (K) and damping ($\xi$). Both stiffness and damping increase with increasing compression. Thus, the vibration amplitudes should increase for taller spring heights and decrease for shorter heights.

The analytical model predicts the vibration amplitudes fairly well for the 4-inch and higher compressed heights. However, the amplitudes obtained for the 3.7-inch and 3.3-inch spring heights are much smaller than predicted. This indicates the spring does not necessarily respond in the same manner as a single circular cylinder to the vortex shedding vibration mechanism. As the spring is compressed, the spacing between coils is reduced. Apparently, when the coils are brought close enough together, the vortices shed from an upstream coil run into the next coil, thus breaking up and preventing further vortex formation.

Pitch-to-diameter ratios calculated for the compressed heights tested are listed in Table 2. The pitch corresponds to the longitudinal (flow direction) distance between the centerlines of adjacent coils. The diameter is the wire diameter. In the region of a 2.0 pitch-to-diameter ratio, the amplitude at the Strouhal frequency tends to diminish. Although an increased amplitude was observed in this region, as shown in Figure 5, the large resonance vibration of the higher compressed heights did not occur. Below the 2.0 ratio, the resonance amplitude was totally suppressed. Studies on three additional spring designs also indicate that at a pitch-to-diameter ratio of approximately 2.0, the increased amplitude associated with vortex shedding either does not occur or is negligible.

### 4.2 Alternate Designs

Four additional spring designs (see Table 1) were flow tested. The major changes among the springs were wire diameter, mean diameter, number of coils, and free height. The changes affected the spring stiffnesses and natural frequencies. The frequencies of Spring No. 2 were nearly the same as those of Spring No. 1. The natural frequencies of Springs No. 3, No. 4, and No. 5 were consecutively higher.

Figure 6 shows the amplitude response of the additional springs as a function of flow velocity at the 4-inch compressed height. These springs exhibit the same flow response characteristics as the reference spring in which the coil amplitudes peaked when the Strouhal frequency coincided with the spring natural frequency. The large amplitude vortex shedding occurred for Spring No. 2. The response amplitudes of Springs No. 3, No. 4, and No. 5 generally increased as a function of velocity squared. Broad peaks in the vicinity of the Strouhal-natural frequency lock-in region suggest vortex shedding for Springs No. 3 and No. 4. However, the Reynolds numbers for these springs exceed $10^5$. In this region, the Strouhal number is not well defined, and vortex shedding may or may not occur.

## 5. Conclusions

Helical coil compression springs installed in a flowing water environment will be subject to flow-induced vibration. The vibration amplitude may be large or small depending on the operating conditions and the spring characteristics.

The helical coil springs respond in a similar manner as a single circular cylinder in cross-flow. Two FIV excitation mechanisms cause the spring to vibrate. Small amplitude vibrations which increase as a function of velocity squared are due to turbulent buffeting. Large amplitude vibration due to vortex shedding may occur if the Strouhal and natural frequencies coincide.

By calculating the vortex shedding frequencies and velocities, the designer can determine if his spring will operate without large amplitude vibration. Design modifications can be made to separate vortex shedding frequencies and spring structural frequencies. Stiffness and natural frequency characteristics of the spring can be adjusted by modifying the wire diameter, mean diameter free height, and number of coils to provide an adequate margin to resonance.

## REFERENCES


[1] R. D. BLEVINS, Flow-Induced Vibration, Van Nostrand Reinhold, New York, 1977.

[2] Y. S. SHIN and M. W. WAMBSGANSS, "Flow-Induced Vibration in LMFBR Steam Generators: A State-of-the-Art Review," Nuclear Engineering and Design, 40, 1977.

[3] J. H. LEINHARD, "Synopsis of Lift, Drag, and Vortex Frequency Data for Rigid Circular Cylinders," Washington State University Bulletin 300, 1966.


Table 1 Spring Specifications

| Spring Design | Free Height (in) | Solid Height (in) | Spring Rate (lb/in) | Wire Diameter (in) | Mean Diameter (in) | Active Coils | Active Coils |
|---|---|---|---|---|---|---|---|
| 1 | 7.2 | 2.2 | 93 | .34 | 3.38 | 5.2 | 6.9 |
| 2 | 7.6 | 2.8 | 121 | .38 | 3.41 | 5.5 | 7.2 |
| 3 | 5.2 | 2.2 | 180 | .38 | 3.38 | 4.0 | 5.7 |
| 4 | 4.9 | 2.2 | 221 | .38 | 3.38 | 3.2 | 5.0 |
| 5 | 4.8 | 2.4 | 272 | .38 | 3.38 | 2.6 | 6.5 |

Shear Modulus $11.5 \times 10^6$ psi

Material Density .25 $lb/in^3$

Table 2 Spring No. 1 Pitch-to-Diameter Ratios

| Compressed Height (inches) | P/D |
|---|---|
| 4.9 | 2.8 |
| 4.6 | 2.5 |
| 4.3 | 2.35 |
| 4.0 | 2.2 |
| 3.7 | 2.0 |
| 3.3 | 1.7 |

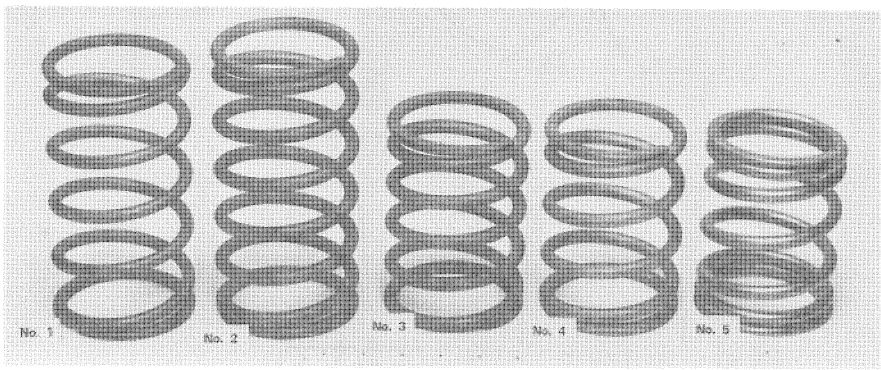


Figure 1 Helical Coil Springs Tested

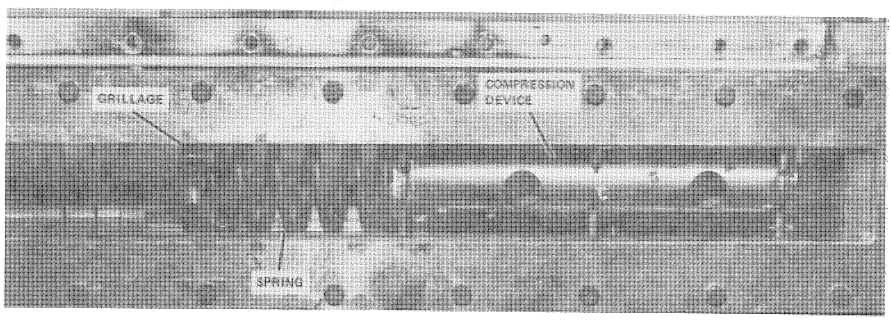


Figure 2 Flow Channel

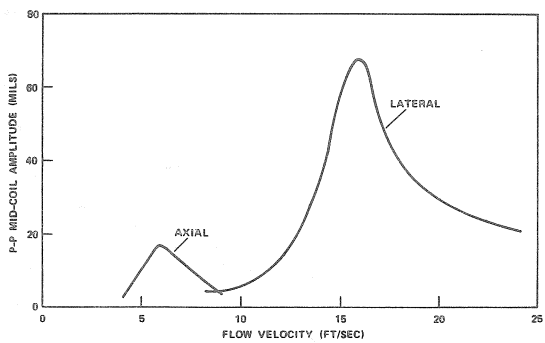


Figure 3 Spring No. 1 Flow Response

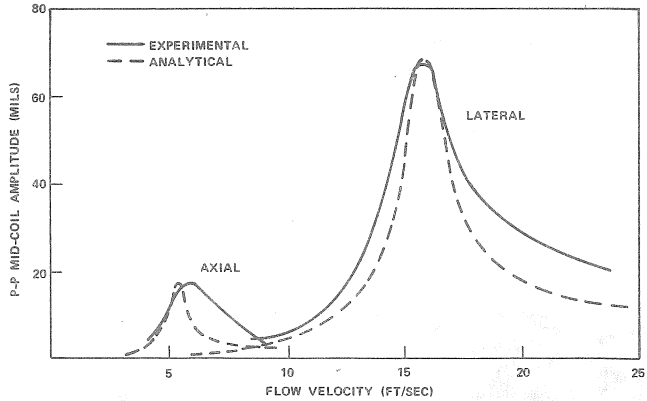


Figure 4 Spring No. 1 Analytical - Experimental Comparison

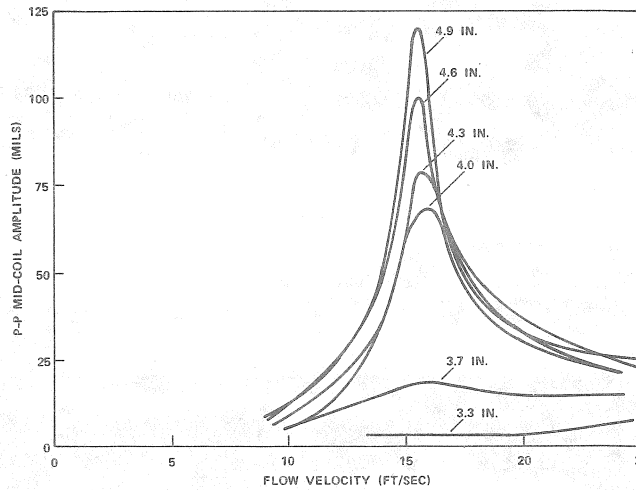


Figure 5 Spring No. 1 Compressed Height Effects

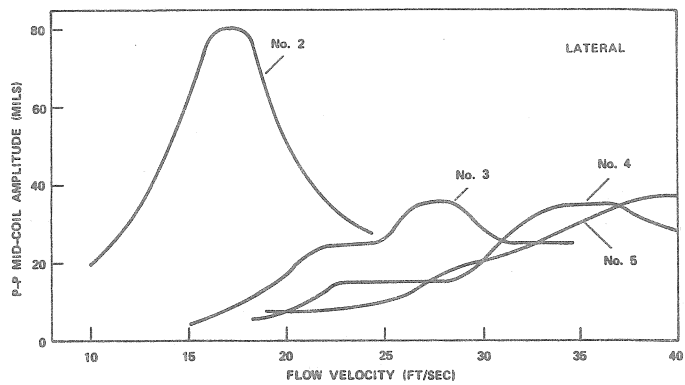


Figure 6 Alternate Design Flow Response